3. Chute JP, Chen T, Feigal E et al. Twenty years of phase III trials for patients with extensive-stage small-cell lung cancer: perceptible progress. J Clin Oncol 1999; 17: 1794–1801.
4. Schilsky RL. End points in cancer clinical trials and the drug approval process. Clin Cancer Res 2002; 8: 935–938.
5. Saijo N. Strategy for the development of novel anticancer drugs. Cancer Chemother Pharmacol 2003; 52 (Suppl 1): S97–S101.
6. Stahel RA, Ginsberg R, Havemann K et al. Staging and prognostic factors in small cell lung cancer: a consensus report. Lung Cancer 1989; 5: 119–126.
7. Zelen M. Keynote address on biostatistics and data retrieval. Cancer Chemother Rep 3 1973; 4: 31–42.
8. Chu T-M, Weir B, Wolfinger R. A systematic statistical linear modeling approach to oligonucleotide array experiments. Math Biosci 2002; 176: 35–51.
9. van den Bent MJ. The role of chemotherapy in brain metastases. Eur J Cancer 2003; 39: 2114–2120.
10. Hotta K, Matsuo K, Ueoka H et al. Continued gefitinib treatment after disease stabilisation prolongs survival of patients with non-small-cell lung cancer: Okayama Lung Cancer Study Group Experience. Ann Oncol 2005; 16: 1817–1823.
11. Hotta K, Kiura K, Toyooka S et al. Clinical significance of epidermal growth factor receptor gene mutations on treatment outcome after first-line cytotoxic chemotherapy in Japanese patients with non-small-cell lung cancer. J Thorac Oncol 2007; 2: 632–637.
12. Hotta K, Kiura K, Takigawa N et al. Sex difference in the influence of smoking status on the responsiveness to gefitinib monotherapy in adenocarcinoma of the lung: Okayama Lung Cancer Study Group Experience. J Cancer Res Clin Oncol 2009; 135(1): 117–123.
13. Johnson KR, Ringland C, Stokes BJ et al. Response rate or time to progression as predictors of survival in trials of metastatic colorectal cancer or non-small-cell lung cancer: a meta-analysis. Lancet Oncol 2006; 7: 741–746.
14. Berlin JA, Santanna J, Schmid CH et al. Individual patient-versus group-level data meta-regressions for the investigation of treatment effect modifiers: ecological bias rears its ugly head. Stat Med 2002; 21: 371–387.
15. Slotman B, Faivre-Finn C, Kramer G et al. Prophylactic cranial irradiation in extensive small-cell lung cancer. N Engl J Med 2007; 357: 664–672.

Prognosis of Small Adenocarcinoma of the Lung Based on Thin-Section Computed Tomography and Pathological Preparations

Mizuki-Ikehara, MD, Haruhiro Saito, MD,† Kouzo Yamada, MD,† Fumihiro Oshita, MD,† Kazumasa Noda, MD,† Haruhiko Nakayama, MD,† Kazuo Masui, MD,‡ Yoichi Kameda, MD,‡ Yuko Komase, MD,* and Teruomi Miyazawa, MD,**

Objective: We investigated the relationship between findings from tumor opacity in the mediastinal window image and solid lesions in pathological preparations and related the results to tumor recurrence.

Methods: The subjects were 115 patients with a lung adenocarcinoma of 20 mm or smaller who underwent surgical resection. The proportion of the reduction in the tumor opacity in the mediastinal window image maximum diameter to the maximum diameter of the tumor opacity was calculated as the reduction percentage, and the proportion of the maximum solid lesions in pathological preparation diameter to the maximum tumor diameter was calculated as the pathological ratio.

Results: The incidence of relapse was significantly higher in patients with a reduction percentage of less than 50% and in patients with a pathological ratio of less than 50%.

Conclusions: Measurement of the reduction percentage and the pathological ratio may allow prediction of prognosis of small adenocarcinoma of the lung.

Key Words: small adenocarcinoma, lung, thin-section CT, solid lesion, prognosis

(*J Comput Assist Tomogr* 2008;32:426–431)

Early detection and early treatment of lung cancer is of importance to improve therapeutic outcomes. Introduction of computed tomography (CT) screening and advancement of diagnostic CT imaging have enabled early detection and early diagnosis of small peripheral-type lung cancers,[1] and such cases are mostly adenocarcinoma. The potential to diagnose and treat peripheral small adenocarcinoma is likely to increase, and qualitative diagnosis is important for establishment of therapeutic policies. Although a small diameter is one of the characteristics of early cancers, a subgroup of small peripheral-type lung cancers are already invasive despite early detection. Patz et al[2] reported that the tumor diameter is not correlated with disease extent or prognosis of small lung cancers of 30 mm or less in diameter, suggesting that other criteria are necessary for prediction of prognosis of peripheral-type early cancers. The current standard therapy for peripheral-type lung adenocarcinoma is lobectomy with lymph node dissection if applicable. However, a subgroup of cases with small adenocarcinoma of the lung have a good prognosis even with limited surgery, and if the prognostic factors in early cancer could be defined, the indication for limited surgery may expand.

A study performed at Kanagawa Cancer Center previously found that the tumor opacity in the mediastinal window image (TOM) of thin-section CT (TS-CT) is associated with the prognosis of patients with lung adenocarcinoma of 20 mm or smaller in diameter.[3,4] However, the pathology of the TOM has not been fully investigated; therefore, in this study, we examined whether TS-CT findings reflect pathological findings in detail and determined the association of tumor opacity with prognosis.

MATERIALS AND METHODS

This study was approved by the institutional Review Boards of Kanagawa Cancer Center and St. Marianna University School of Medicine. Informed consent was obtained from each patient before operation. The subjects were 115 patients with peripheral-type adenocarcinoma of the lung who underwent surgical resection at the Kanagawa Cancer Center between January 1997 and October 2003. Patients with bronchioloalveolar carcinoma (BAC) undetectable in the mediastinal window image were excluded. Contrast-enhanced CT scans were performed using an Aquilion M/16 or X-Vigor/Real system (Toshiba Medical Systems, Tokyo, Japan). High-resolution images targeted to the tumor were obtained at 120 kV (peak) and 200 mA using sections of 2-mm thickness. Images were photographed on each sheet of film using mediastinal (level, 40 Hounsfield unit [HU]; width, 400 HU) and lung (level, −600 HU; width, 1600 HU) window settings.

The findings of TS-CT was evaluated and measured the maximum diameter of the TOM in TS-CT. The proportion of the reduction in the maximum TOM diameter relative to the

From the *Division of Respiratory and Infectious Diseases, Department of Internal Medicine, St Marianna University School of Medicine; †Department of Thoracic Oncology and ‡Pathology, Kanagawa Cancer Center, Yokohama, Japan.

Received for publication March 26, 2007; accepted May 15, 2007.

Reprints: Mizuki Ikehara, MD, Division of Respiratory and Infectious Diseases, Department of Internal Medicine, St. Marianna University School of Medicine, Yasashi-cho 1197-1, Asahi-ku, Yokohama, 241-0811, Japan (e-mail: mizukiikehara@aol.com).

This study was supported in part by a grant from Scientific Research Expenses for Health Labour and Welfare Programs and the Foundation for the Promotion of Cancer Research, and by Second-Term Comprehensive 10-year Strategy for Cancer Control.

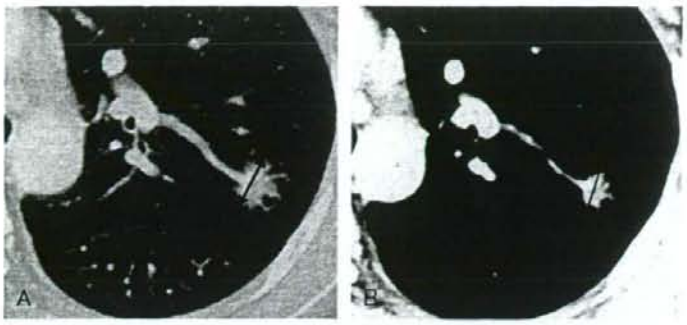

FIGURE 1. Adenocarcinoma with mixed subtypes. TS-CT lung window image (A) and TS-CT mediastinal window image (B). Reduction percentage (%) = {[Tumor diameter (lung window: black arrow) − Tumor diameter (mediastinal window: black line)]/Tumor diameter (lung window)} ×100.

maximum diameter of the tumor opacity in the lung window was calculated as the reduction percentage (Fig. 1).

The excised lung was distended and fixed by infusion of formalin from the bronchus. The specimen including the maximum cross-sectional area of the tumor was sliced into several sections at intervals of a few millimeters and stained with hematoxylin and eosin. The maximum diameter of the solid lesion in the pathological preparation (SLP) observed under a magnifying glass was measured. The SLP was defined as follows: (1) regions with alveolar collapse, (2) regions accompanied by destruction of the alveolar framework, and (3) regions described in (2) accompanied by collagen fibrotic foci. The proportion of the maximum SLP diameter to the maximum tumor diameter in the pathological preparation was calculated as the pathological ratio (Fig. 2).

Comparisons between the maximum diameters of the tumor opacity in the lung window in TS-CT and the maximum diameters in the pathological preparation, between the maximum TOM and SLP diameters, and between the reduction percentage and pathological ratio were performed using Pearson correlation coefficient.

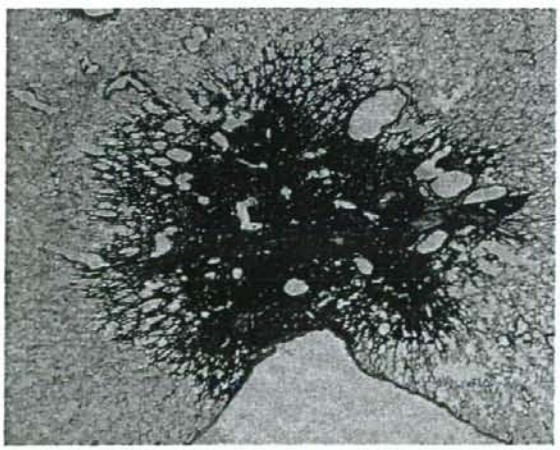

FIGURE 2. Adenocarcinoma with mixed subtypes. Pathological ratio (%) = {[Tumor diameter (black line) − Maximum diameter of solid lesion (black arrow)]/Tumor diameter} ×100.

To investigate the association with prognosis, the relationships of relapse with the maximum TOM and SLP diameters, reduction percentage, and pathological ratio were analyzed by the Kaplan-Meier method and subjected to log-rank tests.

RESULTS

The background characteristics of the patients are shown in Table 1. The patients comprised 52 men and 63 women and had a median age of 67 years. The disease stage was Ia in 95 patients, Ib in 10, IIa in 2, IIb in 3, IIIa in 4, and IIIb in 1, and cancer recurred in 16 patients (13.9%). Of the 115 patients, 99 patients underwent lobectomy with systemic hilar and mediastinal lymph node dissection, whereas 16 patients underwent wedge resection. There were no recurrences in patients who underwent wedge resection. None of the cases had been treated by radiotherapy or chemotherapy.

Pathological findings are shown in Table 2. All cases included alveolar collapse, destruction of the alveolar framework, or collagen fibrotic foci. The histological types were determined according to the World Health Organization classification: the tumor was of the acinar type in 1 case, papillary type in 8, BAC in 12, adenocarcinoma with mixed subtypes in 80, and solid adenocarcinoma with mucin in 14. The Noguchi classification[5] was type B (localized BAC [LBAC] with foci of structural collapse of alveoli) in 12 cases, type C (LBAC with foci of active fibroblastic proliferation) in 80, type D (poorly differentiated adenocarcinoma) in 14, type E (tubular adenocarcinoma) in one, and type F (papillary adenocarcinoma with a compressive growth pattern) in 8. Lymphatic invasion was noted in 21

TABLE 1. Patient Characteristics

Characteristic	No.
No. patients	115
Sex (male/female)	52/63
Age (median, range)	67 (29–82)
p-stage	
I (Ia/Ib)	95/10
II (IIa/IIb)	2/3
III (IIIa/IIIb)	4/1
Relapse	16

TABLE 2. Pathological Findings

	No. (%)
Subtypes of adenocarcinoma	
Acinar	1 (0.9)
Papillary	8 (7.0)
BAC	12 (10.4)
Adenocarcinoma with mixed subtypes	80 (69.6)
Solid adenocarcinoma with mucin	14 (12.1)
Noguchi classification	
Type B	12 (10.4)
Type C	80 (69.6)
Type D	14 (12.1)
Type E	1 (0.9)
Type F	8 (7.0)
Lymphatic permeation	21 (18.3)
Vascular invasion	33 (28.7)
Pleural involvement	17 (14.8)
Nodal involvement	9 (7.8)

Type A indicates LBAC; type B, LBAC with foci of structural collapse of alveoli; type C, LBAC with foci of active fibroblastic proliferation; type D, poorly differentiated adenocarcinoma; type E, tubular adenocarcinoma; type F, papillary adenocarcinoma with a compressive growth pattern.

cases (18.3%), vascular invasion in 33 (28.7%), pleural invasion in 17 (14.8%), and lymph node metastasis in 9 (7.8%).

Tumor diameter-related parameters are shown in Table 3. In TS-CT findings, the median tumor diameter was 18 mm, the median maximum TOM diameter was 12 mm, and the median reduction percentage was 25%. In the pathological preparation, the median tumor diameter was 14 mm, the median maximum SLP diameter was 10 mm, and the median pathological ratio was 24.1%. An analysis of the correlation between the TS-CT and pathological findings gave correlation coefficients of 0.714 ($P < 0.0001$) for the relationship between the maximum diameter of the tumor opacity in the lung window and the pathological maximum tumor diameter, 0.874 ($P < 0.0001$) for the relationship between the maximum TOM and SLP diameters, and 0.903 ($P < 0.0001$) for the relationship between the reduction percentage and pathological ratio.

Analysis of the association of relapse with the maximum TOM and SLP diameters, reduction percentage,

TABLE 3. Maximum Diameters in TS-CT and in Pathological Preparations and the Reduction Percentage and Pathological Ratio (n = 115)

	Size, mm
TS-CT	
Tumor diameter in lung window images, median (range)	18 (8–28)
Tumor diameter in mediastinal window images, median (range)	12 (1–22)
Reduction percentage, median (range)	25 (0–88.9)
Pathological preparation	
Pathological tumor diameter, median (range)	14 (4–20)
Maximum diameter of solid lesions, median (range)	10 (1–20)
Pathological ratio, median (range)	24.1 (0–84.5)

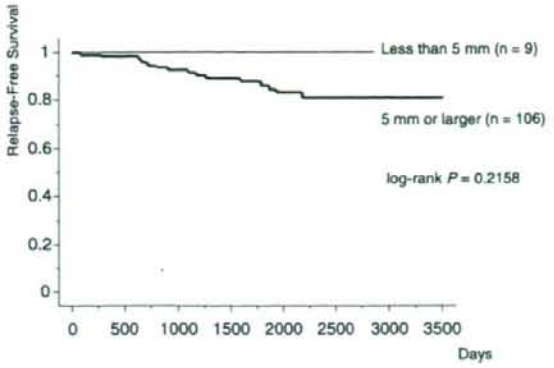

FIGURE 3. Maximum TOM diameter in TS-CT and relapse-free survival.

and pathological ratio gave the following results. Relapse did not occur in patients with a maximum TOM diameter of less than 5 mm, but the difference in incidence of relapse between these patients and those with a maximum TOM diameter of 5 mm or greater was not significant by log-rank test (Fig. 3). The maximum TOM diameter was less than 5 mm in 9 cases, accounting for 7.8% of all cases. Statistically, no significant difference was noted in the incidence of relapse examined at various cutoff values with maximum TOM diameter. However, the incidence of relapse was significantly higher in patients with a reduction percentage of less than 50% compared with those with a reduction percentage of 50% or greater (log-rank test, $P = 0.0203$); no relapse occurred in patients with a reduction percentage of 50% or greater (Fig. 4). No relapse was prominent for in the 28 cases with a reduction percentage of 50% or greater, which accounted for 24.3% of all cases. Regarding the pathological preparations, relapse occurred in only 1 patient with a maximum SLP diameter of less than 5 mm, but there was no significant difference in the incidence of relapse between patients with maximum SLP diameters of less than 5 mm and 5 mm or greater (Fig. 5). The maximum SLP diameter was less than 5 mm in 15 cases, accounting for 13.0% of all cases. Statistically, there was no

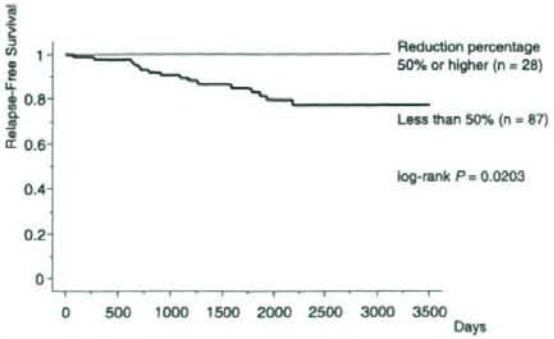

FIGURE 4. Reduction percentage in TS-CT and relapse-free survival.

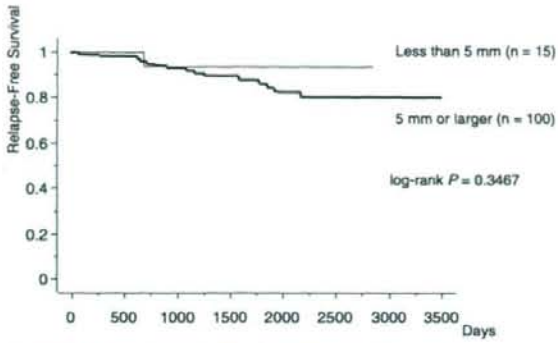

FIGURE 5. Maximum SLP diameter in pathological preparations and relapse-free survival.

significant difference in the incidence of relapse examined at various cutoff values with the maximum SLP diameter. However, the incidence of relapse was significantly higher in patients with a pathological ratio of less than 50% compared with those with a pathological ratio of 50% or greater (log-rank test, $P = 0.0493$); no relapse occurred in patients with a pathological ratio of 50% or greater (Fig. 6). No relapse occurred in the 20 cases with a pathological ratio of 50% or greater, which accounted for 17.4% of all cases.

No acinar, papillary, or solid adenocarcinoma with mucin subtype was noted pathologically when the reduction percentage and pathological ratio exceeded 50%, nor was there vascular, lymphatic, or pleural invasion or lymph node metastasis in such cases (Tables 4 and 5).

DISCUSSION

A previous report from Kanagawa Cancer Center showed that cases of lung adenocarcinoma of 20 mm or smaller in diameter can be divided into 2 groups with different prognoses, based on the reduction percentage of the area in the mediastinal window image in TS-CT compared with the area in the peripheral window image in TS-CT being 50% or greater (air-containing type) and less than 50% (solid-density type).[3,4] Relapse did not occur in patients with tumors

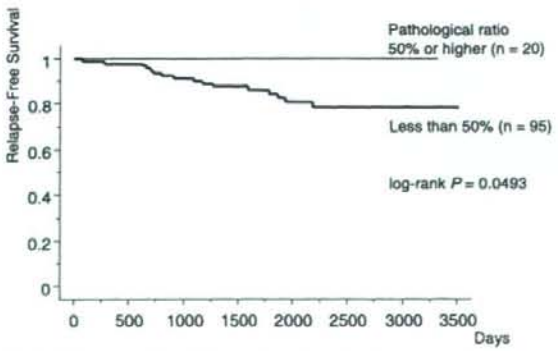

FIGURE 6. Pathological ratio in pathological preparations and relapse-free survival.

TABLE 4. Relationship Between a Reduction Percentage of Less Than 50% in TS-CT and the Pathological Findings

	Reduction Percentage ≥50% (n = 28)	Reduction Percentage <50% (n = 87)
Subtypes of adenocarcinoma		
Acinar	0	1
Papillary	0	8
BAC	8	4
Adenocarcinoma with mixed subtypes	20	60
Solid adenocarcinoma with mucin	0	14
Noguchi classification		
Type B	8	4
Type C	20	60
Type D	0	14
Type E	0	1
Type F	0	8
Lymphatic permeation	0	21
Vascular invasion	0	33
Pleural involvement	0	17
Nodal involvement	0	9

of the air-containing type, whereas recurrence was noted in approximately 25% of solid-density type cases, suggesting that a reduction percentage of 50% or greater is a positive prognostic factor. Tumors of the air-containing type belonged to BAC, whereas tumors of the solid-density type belonged to acinar, papillary, adenocarcinoma with mixed subtypes, or solid adenocarcinoma with mucin. Evaluation of the reduction percentage in the major axis of the tumor, which is a simpler approach, may also be a positive prognostic factor. In this study, we investigated the pathological validity of these

TABLE 5. Relationship Between a Pathological Ratio of Less Than 50% in the Pathological Preparation and Pathological Findings

	Pathological Ratio ≥50% (n = 20)	Pathological Ratio <50% (n = 95)
Subtypes of adenocarcinoma		
Acinar	0	1
Papillary	0	8
BAC	8	4
Adenocarcinoma with mixed subtypes	12	68
Solid adenocarcinoma with mucin	0	14
Noguchi classification		
Type B	8	4
Type C	12	68
Type D	0	14
Type E	0	1
Type F	0	8
Lymphatic permeation	0	21
Vascular invasion	0	33
Pleural involvement	0	17
Nodal involvement	0	9

imaging studies by comparing the maximum diameters of tumor opacity in the lung window (TOM) and the reduction percentage in TS-CT with the maximum diameters of the tumor (SLP) and the pathological ratio in the pathological preparation.

The air-containing category includes ground-glass opacity (GGO) tumors whose reduction percentage is 100%; GGO tumors have been identified as BAC with good prognosis.[6–10] Actually, relapse did not occur in all 53 cases with a reduction percentage of 100% that underwent surgical resection at Kanagawa Cancer Center between January 1997 and October 2003. Therefore, we excluded these cases. With exclusion of GGO tumors, differentiation of lesions into good and poor prognosis groups using TS-CT may be useful,[11] but the prognostic factors have not been fully investigated. Based on Pearson correlation coefficients, our data suggest a strong relationship between TS-CT findings and pathological findings for the relationships between the maximum TOM and SLP diameters and between the reduction percentage and pathological ratio. However, the relationship between the maximum tumor diameters in the TS-CT image and pathological preparation was slightly weaker. These findings suggest that the tumor opacity in the TS-CT mediastinal window faithfully reflects the SLP. The correlation coefficient between the reduction percentage and the pathological ratio was particularly high, showing that contrasting the mediastinal window image with the lung window image faithfully reflects the pathological findings. We note that slicing the excised lung in the same direction as that used for CT is difficult, and alteration of the size of air-containing lesions by formalin fixation is likely; however, the influence of these variables on the relationship between the reduction percentage and pathological ratio seems to be negligible.

Suzuki et al[12] and Yokose et al[13] have reported that the maximum diameter of the central scar may be associated with the prognosis of lung adenocarcinoma of 30 mm or lesser in diameter; these studies indicated that carcinoma did not recur, and qualitative diagnosis of cancer was possible in cases with a central scar diameter of 5 mm or smaller.

Definitions differ in SLP and the central scar. However, in our patients, recurrence did occur in some cases, although the maximum SLP diameter was 4 mm, suggesting that the maximum SLP diameter alone is insufficient for judgment of good prognosis (Fig. 7). The recurrent cases were solid adenocarcinoma with mucin, which did not show a lepidic growth pattern. Because the incidence of relapse is high in this type, the maximum SLP diameter may not serve as a prognostic factor.[5] In fact, there was no significant difference in the incidence of relapse between cases with a maximum SLP diameter of 5 mm or greater and less than 5 mm. In contrast, there was a significant difference in the incidence of relapse between cases with a pathological ratio of 50% or greater and less than 50%. These findings suggest that the pathological ratio may be more useful than the maximum SLP diameter for prediction of relapse.

In TS-CT, there was no significant difference in the incidence of relapse between cases with a maximum TOM diameter of 5 mm or greater and less than 5 mm. Although a significant difference was found in the incidence of relapse between cases with a reduction percentage of 50% or greater and less than 50%. Ohde et al[14] have reported that the prognosis was significantly better when the major axis of the tumor consolidation on the lung window image in TS-CT was 50% or less of the entire tumor diameter, and our results suggest that the reduction percentage is more useful than the maximum TOM diameter for prediction of relapse.

The pathological examination indicated that the solid lesions were the following: (1) regions with alveolar collapse, (2) regions accompanied by destruction of the alveolar framework, and (3) regions described in (2) that were accompanied by collagen fibrotic foci. Noguchi et al[5] classified the histopathology of small adenocarcinoma of the lung and found that destruction of the alveolar framework and collagen fibrotic foci were associated with prognosis; therefore, solid lesions in the pathological preparation may have contained a region associated with invasiveness of lung adenocarcinoma. Goto et al[15] reported that prognosis varied depending on the condition of the alveolar framework in lung adenocarcinoma of 20 mm or smaller in diameter and that prognosis was significantly poorer in cases with destruction of the alveolar framework associated with destruction of the basement membrane, suggesting that destruction of the basement membrane is the first step in tumor invasion. Because tumor invasion is accompanied by destruction of the alveolar framework and collagen fibrosis, the alveolar air space may be lost, resulting in formation of a solid region in the pathological preparation.

A lepidic growth and advancement pattern of the adenocarcinoma was noted in 80% of our cases, supporting the hypothesis that the early stage of lung adenocarcinoma is often BAC. In this growth and advancement pattern, the air-containing region is initially retained because the lesion

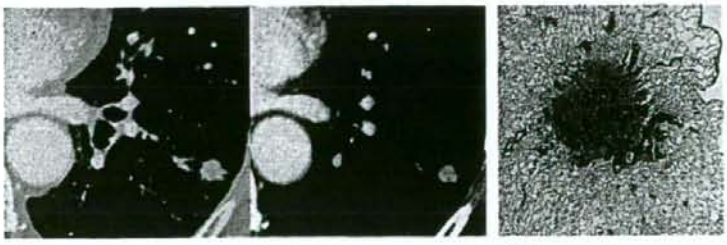

A B

FIGURE 7. A recurrent case with a maximum SLP diameter of 4 mm. Solid adenocarcinoma with mucin: TS-CT (A); pathological preparation (B).

grows by replacement of alveolar lining cells, but acquisition of invasiveness is accompanied by destruction of the alveolar framework and collagen fibrosis, which decreases the air-containing region and increases the solid region. Therefore, decreases in the reduction percentage and pathological ratio may represent a state in which increased invasiveness has caused a decreased air-containing region and an increased solid region. Acinar, papillary, or solid adenocarcinoma with mucin are tumors with nonlepidic growth pattern, and prognosis of them is worse than tumors with lepidic growth pattern (BAC).[5] Pathological ratio and reduction percentage of tumors with nonlepidic growth pattern were less than 50% (Tables 4 and 5).

The correlation coefficient between the reduction percentage in TS-CT and the pathological ratio was very high, and no relapse occurred in cases with a reduction percentage exceeding 50%, confirming that the reduction percentage accurately reflects the pathological findings. Therefore, use of the reduction percentage in TS-CT to roughly divide lesions into 2 groups with different prognoses may be valid based on the pathological investigation. Measurements of the reduction percentage and pathological ratio may allow identification of lung adenocarcinoma with good prognosis. Such measurements are straightforward during intraoperative rapid diagnosis and may be useful for prediction of relapse and judgment of the indication for clinical treatment of early cancer. These findings suggest that prospective investigations of the indications for limited surgery and postoperative adjuvant therapy should be performed for small adenocarcinoma of the lung.

REFERENCES

1. Henschke CI, McCauley DI, Yankelevitz DF, et al. Early Lung Cancer Action Project: overall design and findings from baseline screening. *Lancet*. 1999;354:99–105.
2. Patz EF, Goodman PC, Bepler G. Screening for lung cancer. *N Engl J Med*. 2000;343:1627–1633.
3. Kondo T, Yamada K, Noda K, et al. Radiologic-prognostic correlation in patients with small pulmonary adenocarcinomas. *Lung Cancer*. 2002;36:49–57.
4. Shimizu K, Yamada K, Saito H, et al. Surgically curable peripheral lung carcinoma: correlation of thin-section CT findings with histologic prognostic factors and survival. *Chest*. 2005;127:871–878.
5. Noguchi M, Morikawa A, Kawasaki M, et al. Small adenocarcinoma of the lung. Histologic characteristics and prognosis. *Cancer*. 1995;75:2844–2852.
6. Aoki T, Nakata H, Watanabe H, et al. Evolution of peripheral lung adenocarcinomas: CT findings correlated with histology and tumor doubling time. *AJR Am J Roentgenol*. 2000;174:763–768.
7. Kuriyama K, Seto M, Kasugai T, et al. Ground-glass opacity on thin-section CT: value in differentiating subtypes of adenocarcinoma of the lung. *AJR Am J Roentgenol*. 1999;173:465–469.
8. Yang ZG, Sone S, Takashima S, et al. High-resolution CT analysis of small peripheral lung adenocarcinomas revealed on screening helical CT. *AJR Am J Roentgenol*. 2001;176:1399–1407.
9. Jang HJ, Lee KS, Kwon OJ, et al. Bronchioloalveolar carcinoma: focal area of ground-glass attenuation at thin-section CT as an early sign. *Radiology*. 1996;199:485–488.
10. Nakajima R, Yokose T, Kakinuma R, et al. Localized pure ground-glass opacity on high-resolution CT: histologic characteristics. *J Comput Assist Tomogr*. 2002;26:323–329.
11. Kodama K, Higashiyama M, Yokouchi H, et al. Prognostic value of ground-glass opacity found in small lung adenocarcinoma on high-resolution CT scanning. *Lung Cancer*. 2001;33:17–25.
12. Suzuki K, Yokose T, Yoshida J, et al. Prognostic significance of the size of central fibrosis in peripheral adenocarcinoma of the lung. *Ann Thorac Surg*. 2000;69:893–897.
13. Yokose T, Suzuki K, Nagai K, et al. Favorable and unfavorable morphological prognostic factors in peripheral adenocarcinoma of the lung 3 cm or less in diameter. *Lung Cancer*. 2000;29:179–188.
14. Ohde Y, Nagai K, Yoshida J, et al. The proportion of consolidation to ground-glass opacity on high resolution CT is a good predictor for distinguishing the population of non-invasive peripheral adenocarcinoma. *Lung Cancer*. 2003;42:303–310.
15. Goto K, Yokose T, Kodama T, et al. Detection of early invasion on the basis of basement membrane destruction in small adenocarcinomas of the lung and its clinical implications. *Mod Pathol*. 2001;14:1237–1245.

Lung Cancer (2008) 62, 45–54

available at www.sciencedirect.com

ScienceDirect

journal homepage: www.elsevier.com/locate/lungcan

Megakaryocyte potentiating factor as a tumor marker of malignant pleural mesothelioma: Evaluation in comparison with mesothelin

Kota Iwahori[a,b], Tadashi Osaki[a,*], Satoshi Serada[b], Minoru Fujimoto[b], Hidekazu Suzuki[c], Yoshiro Kishi[d], Akihito Yokoyama[e], Hironobu Hamada[f], Yoshihiro Fujii[d], Kentaro Yamaguchi[g], Tomonori Hirashima[c], Kaoru Matsui[c], Isao Tachibana[a], Yusuke Nakamura[h], Ichiro Kawase[a], Tetsuji Naka[b]

[a] *Department of Respiratory Medicine, Allergy, and Rheumatic Diseases, Osaka University Graduate School of Medicine, 2-2 Yamada-oka, Suita, Osaka 565-0871, Japan*
[b] *Laboratory for Immune Signal, National Institute of Biomedical Innovation, 7-6-8 Saito-Asagi, Ibaraki, Osaka 567-0085, Japan*
[c] *Department of Thoracic Malignancy, Osaka Prefectural Medical Center for Respiratory and Allergic Diseases, 3-7-1 Habikino, Habikino, Osaka 583-8588, Japan*
[d] *Department of Research and Development, Ina Institute, Medical & Biological Laboratories, Co., Ltd., 1063-103 Terasawaoka, Ina, Nagano 396-0002, Japan*
[e] *Department of Hematology and Respiratory Medicine, Kochi University, 185-1, Okohchou-kohatu, Nanngoku, Kohchi 783-8505, Japan*
[f] *Department of Integrated Medicine and Informatics, Ehime University Graduate School of Medicine, Sizukawa, Ohonn, Ehime 791-0295, Japan*
[g] *Department of Product Development, Ina Institute, Medical & Biological Laboratories, Co., Ltd., 1063-103 Terasawaoka, Ina, Nagano 396-0002, Japan*
[h] *Laboratory of Molecular Medicine, Human Genome Center, Institute of Medical Science, The University of Tokyo, 4-6-1 Shirokanedai, Minato-ku, Tokyo 108-8639, Japan*

Received 30 October 2007; received in revised form 30 January 2008; accepted 14 February 2008

KEYWORDS
Mesothelioma;
Megakaryocyte potentiating factor;
Mesothelin;
Tumor markers

Summary
Purpose: An early and reliable blood test is one deficiency in diagnosis of malignant pleural mesothelioma (MPM). Megakaryocyte potentiating factor (MPF) and mesothelin variants (MSLN), members of the mesothelin gene family, have been studied as candidate serum markers for MPM. We developed a novel enzyme-linked immunosorbent assay (ELISA) system to compare the diagnostic efficacy of MPF and MSLN in MPM and control groups.
Experimental design: MPF and MSLN were assayed with ELISA in 27 consecutive MPM patients and 129 controls including patients with lung cancer and asymptomatic asbestos-exposed subjects.

Abbreviations: MPM, malignant pleural mesothelioma; MPF, megakaryocyte potentiating factor; MSLN, mesothelin variants 1 and 3; ELISA, enzyme-linked immunosorbent assay.

* Corresponding author. Tel.: +81 6 6879 3833; fax: +81 6 6879 3839.
E-mail address: osaki@imed3.med.osaka-u.ac.jp (T. Osaki).

0169-5002/$ – see front matter
doi:10.1016/j.lungcan.2008.02.012

Results: Statistically significant elevation of serum MPF and MSLN levels was noted in MPM patients in comparison with every control group. The area under the receiver operating characteristic curve (AUC) was calculated for differentiation of MPM and lung cancer, healthy asbestos-exposed subjects, and healthy adults. While the AUC for serum MPF was 0.879, cut-off = 19.1 ng/ml (sensitivity = 74.1%, specificity = 90.4%), the AUC for serum MSLN was 0.713, cut-off = 93.5 ng/ml (sensitivity = 59.3%, specificity = 86.2%). Comparison between AUC for MPF and MSLN values shows that MPF is significantly superior to MSLN ($p = 0.025$). Finally, there was a significant correlation between MPF and MSLN values for MPM (Pearson's correlation coefficient = 0.77; $p < 0.001$).

Conclusions: These findings suggest that diagnostic value of MPF for MPM was better than that of MSLN although both markers showed almost equal specificity for MPM.

1. Introduction

Malignant pleural mesothelioma (MPM) is an aggressive tumor arising from mesothelial cells of serosal cavities. MPM may be asymptomatic at an early stage and is sometimes discovered by routine chest radiography. Common symptoms include chest pain and dyspnea, which are caused by tumor invasion of the chest wall or pleural effusion, and occur late during the disease progression. Although pemetrexed improves survival of unresectable MPM patients, overall median survival is only 12.1 months [1]. MPM is thought to be curable by early radical resection in combination with adjuvant chemoradiotherapy [2]. Even if surgical resection is not applicable, the early use of chemotherapy offers a prolonged period of symptom control and survival. MPM is often associated with past exposure to asbestos. There is a long latency period, often exceeding 20 years, between first exposure to asbestos and diagnosis of MPM [3]. The number of deaths from MPM is expected to increase in the next 20 years in Europe, Japan and Australia, where heavy use of asbestos has occurred [3–6]. There is thus a growing need for sensitive markers that can detect MPM in people at risk for this disease.

A 40-kDa membrane-bound mesothelin and a 31-kDa soluble megakaryocyte potentiating factor (MPF) originate from the same 69-kDa glycosyl-phosphatidylinositol-linked (GPI) glycoprotein precursor [7]. Mesothelin comprises three soluble forms of variants (MSLN). Variant 1 is a predominant mRNA expressed by both normal and tumor cells and its product is detectable in the ascites from ovarian cancer patients. It is thought to be proteolytically cleaved from the cell surface. Soluble variant 3 was detected as a small percentage of total mesothelin products from cell lines and tissues [8,9].

Scholler et al. prepared a monoclonal antibody, OV569, by immunizing mice with ovarian carcinoma cells. OV569 identified a 42- to 45-kDa protein with an N-terminal amino acid sequence identical to that of the membrane-bound portion of mesothelin and MPF, which was designated as soluble mesothelin related proteins (SMRP) [10]. A study utilizing OV569 showed an increase in SMRP concentrations in 37 of 44 patients (84%) with MPM [11]. The commercial assay kit for SMRP is designed to recognize the sequence within membrane-bound mesothelin and thus to measure mesothelin variants 1 and 3 [9]. SMRP is, therefore, identical to MSLN [11].

Later, Shiomi et al. showed that MPF is also secreted into the blood of mesothelioma patients and that the median levels of MPF in those patients were substantially elevated than in those in controls [12]. Onda et al. reported that serum MPF was elevated in 91% (51 of 56) of patients with mesothelioma and that measuring MPF may be useful for monitoring the response of mesothelioma to treatment [13]. Mesothelin variants and MPF thus appear to be promising targets for MPM diagnosis.

However, it has not yet been established whether MPF or MSLN is a more effective marker for differential diagnosis of MPM. To this end, we generated monoclonal antibodies (mAb) and prepared two enzyme-linked immunosorbent assay (ELISA) systems that each recognizes MPF or MSLN. In this paper we report the results of our studies comparing the discriminatory potency of MPF with that of MSLN for diagnosis of MPM.

2. Materials and methods

2.1. Patients and controls

Serum samples were collected from 27 consecutive patients with non-resectable MPM, whose diagnosis was confirmed by cytological or histopathological examination by pathologists skilled in diagnosis of this disease. The patient population included 13 with epithelial type MPM, three with sarcomatoid type, 5 with mixed type and 6 with unclassified type (diagnosed by cytological analysis). For control, we used 47 patients with lung cancer, 35 with other cancers (18 ovarian, 8 stomach and 9 colon cancers), 9 asbestos-exposed asymptomatic subjects and 38 healthy adults without a history of asbestos exposure. We obtained written and oral informed consent from all participants. This study was approved by our institutional review board.

2.2. Antigen preparation

Recombinant MPF protein was produced by amplifying the part coding for amino acids 1–288 from the cDNA encoding the transcript variant 1 for human mesothelin (Genbank accession no. NM_005823) with DNA polymerase

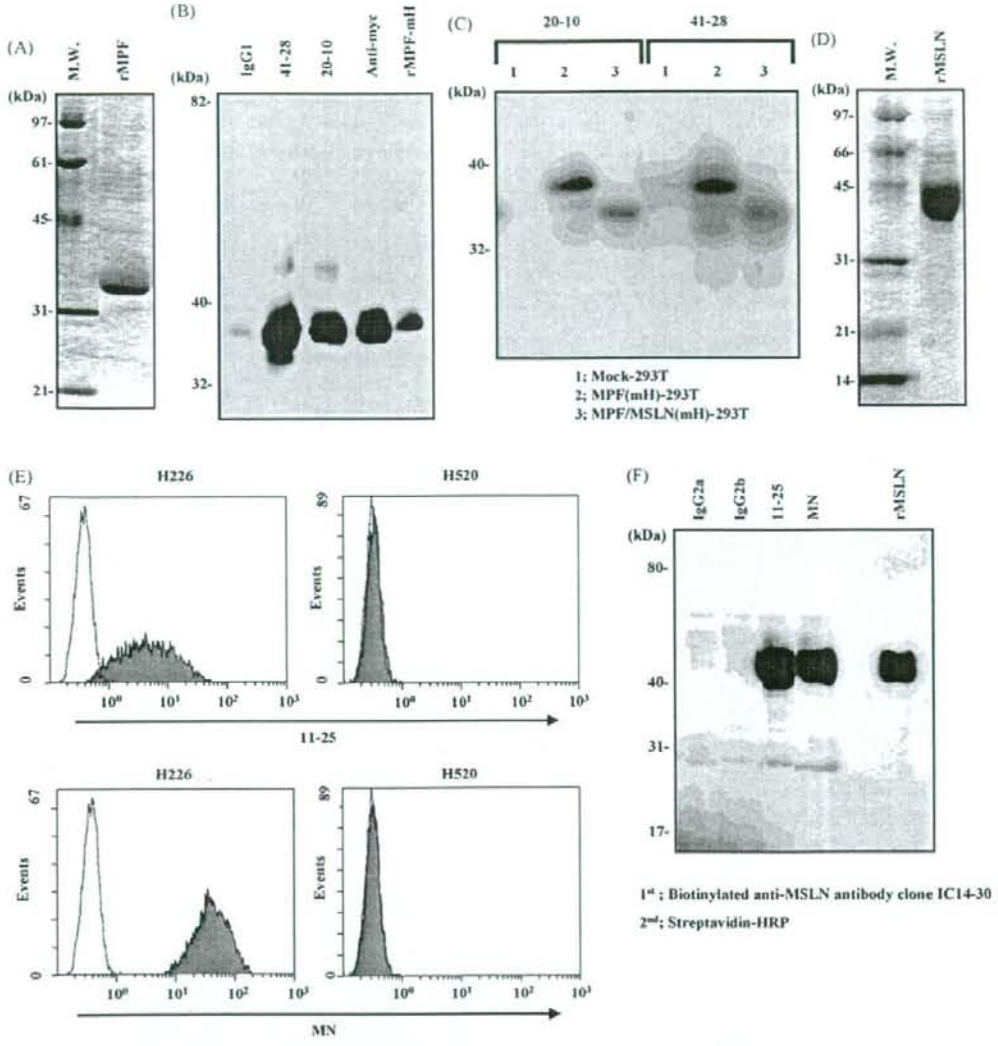

Fig. 1 Characterization of anti-Megakaryocyte potentiating factor (MPF) and anti-mesothelin variants (MSLN) antibodies. (A and D) Purity of the prepared recombinant MPF (A) and MSLN (D) proteins for immunization. Proteins were electrophoresed under reduced condition and stained with Coomassie Brilliant Blue. (B and F) Reactivity of anti-MPF antibodies to recombinant MPF protein (B) or anti-MSLN antibodies to MSLN in the culture supernatant of NCI-H226 cells (F). Anti-MPF antibodies (B, lanes 41–28 and 20–10) or anti-MSLN antibodies (F, lanes 11–25 and MN) were used for immunoprecipitation. Recovered proteins were separated by SDS-PAGE and electrotransfered to polyvinylidenefluoride (PVDF) membranes. Membranes were probed with anti-myc antibody for myc-His tagged MPF or anti-MSLN antibody clone IC14–30 for MSLN, respectively, and followed by development. Recombinant MPF protein (B, lane rMPF-mH) or recombinant MSLN protein (F, lane rMSLN) were applied for positive controls. (C), western blot analysis of anti-MPF antibodies. Supernatants of the HEK 293T transfectants with myc-His tagged MPF, full length of mesothelin variant 1 or mock vectors were separated by SDS-PAGE and electrotransfered to a PVDF membrane. The membrane was probed with anti-MPF antibodies (20–10 and 41–28), incubated with HRP-labeled anti-mouse IgG antibody and followed by chemiluminescence. Lane 1, Mock-transfected 293T; lane 2, myc-His tagged MPF-transfected 293T; lane 3, full length of mesothelin variant 1-transfected 293T. (E), expression of mesothelin on the surface of lung cancer cell lines. NCI-H226 and NCI-H520 were incubated with anti-MSLN antibodies (11–25 and MN) or an isotype-matched control antibody and followed by PE-conjugate anti mouse IgG. Antigen expression was detected by flow cytometry.

(recombinant Taq polymerase; Takara Bio Inc., Shiga, Japan) and using the primers 5′-CGGAATTCGCCGCCACC-ATGGCCTTGCCAACGGCTCGACCCCTGTTG-3′ and 5′-GCTCT-AGAGATGGTCCGTTCAGGCTGCCGCCAGGATGG-3′. The amplified DNA was inserted into the EcoRI/XbaI site of mammalian expression plasmid pcDNA3.1/myc-His (Invitrogen, Carlsbad, CA) and transfected into HEK 293T cells by lipofection (Lipofectamine2000; Invitrogen). The culture supernatant was applied to a TALON resin according to the manufacturer's instructions (Clontech, Mountain View, CA). The purified MPF protein thus obtained was dialyzed with 4.0 liter of PBS twice and kept frozen at −80 °C until use as an immunogen or as a standard polypeptide for sandwich ELISA. Purity of the recombinant MPF was confirmed by Coomassie Brilliant Blue staining after electrophoresis under reduced condition (Fig. 1A).

MSLN was produced by amplifying the part coding for amino acids 297–580 of the same cDNA and using the primers 5′-AAATTTCCCAAGCTTGTGGAGAAGACAGCCTGTCCTTCAG-GCAAG-3′ and 5′-AAGGAAAAAAGCGGCCGCGCCCTGTAGCC-CCAGCCCCAGCGTGTCCAG-3′. The amplified DNA was inserted into the HindIII/NotI site of expression vector pSecTag2B (Invitrogen). It should be noted that variants 1 and 3 of mesothelin share amino acids 297–580 of clone NM_005823 as a common sequence. The plasmid DNA was transfected into HEK 293T cells, and recombinant MSLN produced in the culture supernatant was purified and stored as above (Fig. 1D).

2.3. Antibody generation

To generate mAbs against MPF and against MSLN, 4- to 6-week old BALB/c mice were immunized with the respective purified protein i.p. on days 0, 7, 14, and 16 (10 μg/shot). Following the last immunization, lymphocytes of the spleen were collected and fused with P3U1 myeloma cells in a 50% polyethylene glycol 4000 solution (Wako, Osaka, Japan) on day 18. The fused cells were plated on 96-well plates with RPMI-1640 medium containing 15% fetal calf serum (FCS; Equitech-Bio Inc., Kerrville, TX), penicillin/streptomycin (Invitrogen) and HAT solution (Invitrogen). After 10 days incubation at 37 °C with 5% CO_2 in a humidified environment, culture supernatants were collected and screened for their ability to bind to the immunizing antigen by means of an indirect ELISA using recombinant MPF or soluble mesothelin, respectively. Selected positive hybridoma colonies were expanded and subcloned by limiting dilution. An isostrip kit (Hoffmann-La Roche, Basel, Switzerland) was used for antibody isotype determination according to the manufacturer's instructions. Antibody purification was carried out with protein A affinity chromatography (GE Healthcare, Buckinghamshire, UK). Following a competition assay for the immunogens among the clones thus obtained (data not shown), clone 20–10 (IgG1 κ) and clone 41–28 (IgG1 κ) were selected to construct an sandwich ELISA for the detection of MPF, while MN (IgG2a κ) and 11–25 (IgG2b κ) were chosen for construction of an MSLN ELISA as described elsewhere. Clone MN was previously obtained by Dr. Ira Pastan's laboratory as a specific monoclonal antibody against mesothelin [14] and used in this study under a licensing agreement with NIH. Clones 41–28 and 11–25 were biotinylated using ECL Protein Biotination Module (GE Healthcare).

2.4. Flow cytometry

Lung cancer cell lines NCI-H226 and NCI-H520 were cultured in RPMI medium (SIGMA) supplemented with 10% fetal bovine serum. The former cell line expresses both MPF and MSLN but the latter does neither [14]. After a treatment with PBS containing 5 mM EDTA for 3 min, detached cells were washed with PBS twice and incubated with 1 μg/ml of anti-MSLN Abs or isotype-matched controls for 30 min at 4 °C in PBS containing 0.5% BSA and 2mM EDTA. Following twice wash with the above buffer, PE-conjugate anti-mouse IgG was added and further incubated for 30 min at 4 °C. All flow cytometry was performed on Cytomics FC500 (Beckman Coulter).

2.5. Immunoprecipitation

The reactivity of anti-MPF Abs to recombinant MPF protein, or anti-MSLN Abs to recombinant MSLN protein in the culture supernatant of NCI-H226 was confirmed by immunoprecipitation. 15 μl of Protein G sepharose suspended in PBS containing 0.01% BSA (SIGMA) was incubated with 5 μg of anti-MPF Abs 20–10 and 41–28, or anti-MSLN Abs 11–25 and MN, for 2 h at 4 °C with gently rocking. During this step, 250 ng of the recombinant myc-His tagged MPF protein or 5 times concentrated culture supernatant of NCI-H226 and NCI-H520 were incubated with Protein G beads for 30 min at 4 °C with shaking to preclear the samples. The Protein G sepharose incubated with the antibodies were centrifuged at 1000 × *g* for 2 min and washed with PBS 3 times. Then the precleared samples were added to the tube containing the washed Protein G sepharose and rotated for over night at 4 °C. After the incubation, the beads were washed with PBS 3 times and boiled in 25 μl of 2× Laemmli's SDS sample buffer for 5 min. Proteins (20 μl of sample per lane) were separated by sodium dodecylsulfate-polyacrylamide gel electrophoresis (SDS-PAGE) on a 12.5% polyacrylamide gel and electrotransfered to a polyvinylidenefluoride (PVDF) membrane. The membrane blocked with 5% nonfat milk in PBS containing 0.05% Tween-20 (blocking buffer) was incubated with 1.0 μg/ml mouse anti-myc mAb (MBL) for detecting myc-His tagged MPF, or 1.0 μg/ml biotinylated anti-MSLN antibody clone IC14–30 (MBL) for detecting MSLN for 1 h at room temperature. After 4 times wash with PBS containing 0.05% Tween-20, the membrane was incubated with a horseradish peroxidase (HRP)-conjugated anti-mouse IgG (MBL) for MPF diluted 1:5000 with the blocking buffer or HRP-streptavidin (GE Amersham) for MSLN diluted 1:5000 with the blocking buffer. The chemiluminescence was developed by according to manufacture's procedure (ECL; GE Amersham). 50 ng of recombinant MPF protein or 250 ng of recombinant MSLN protein was applied as a positive control for Western blotting.

2.6. Western blot

HEK 293T cells were transfected by lipofection with expression vectors coding myc-His tagged MPF, full length of

mesothelin variant 1, or a mock vector as a negative control, and the culture media were collected after 72 h-incubation in a CO_2 incubator at 37 °C. Supernatants of the media were recovered by a centrifugation at 3000 × *g* for 10 min at room temperature, and then boiled with an equal volume of 2× SDS sample buffer for 5 min. 20 μl of samples per lane were loaded on a 12.5% SDS-polyacrylamide gel and separated by SDS-PAGE. After electrotransfer to a PVDF membrane, the membrane was treated with the blocking buffer containing 5% nonfat milk and incubated with 2.0 μg/ml anti-MPF Abs (20–10 and 41–28) for 1 h at room temperature. After 4 times wash with PBS containing 0.05% Tween-20, the membrane was incubated with HRP-labeled anti-mouse IgG (MBL) diluted 1:5000 with the blocking buffer. The chemiluminescence was done by according to manufacture's procedure (ECL; GE Amersham).

2.7. Sandwich ELISA

The serum concentrations of MPF and of the soluble form of mesothelin were measured by each specific sandwich ELISA constructed as follows: 96-well microtiter plates (Maxisorp; Nalgen Nunc International Corp., Rochester, NY) were coated with the capturing antibody, clone 20–10 for MPF or clone MN for MSLN, and adjusted to 5 μg/ml with 100 mM carbonate buffer (pH 9.6) at 4 °C overnight. The plates were blocked with 200 μl PBS (pH 7.4) containing 1.0% BSA, 5.0% sucrose, and 0.1% NaN_3 for 2 h and then incubated for 1 h with serum samples diluted to 1:40 with PBS (pH 7.4) containing 1.0% BSA, 0.1% Tween20, 50 μg/ml MAK33 (Roche), and 0.1% NaN_3. After washing with PBS (pH 6.7) containing 0.13% Tween-20, the wells were incubated for 1 h with 2.0 μg/ml biotinylated mAb 41–28 for detecting MPF, or incubated with 0.7 μg/ml biotinylated mAb 11–25 for detecting soluble mesothelin, and reacted with streptavidin-conjugated peroxidase (GE Healthcare) diluted to 1:60,000 for MPF or avidin-conjugated peroxidase (DAKO, Glostrup, Denmark) diluted to 1:10,000 for soluble mesothelin, respectively, with 20 mM HEPES (pH 6.5) containing 1.0% BSA, 0.135 M NaCl, 0.1% *p*-hydroxy phenyl acetic acid (Tokyo Chemical Industry, Tokyo, Japan), and 0.15% ProClin150 (Supelco, St. Louis, MO). Followed by four washes with PBS, 50 μl/well TMB (Moss Inc., Pasadena, MD) was added and the plates were incubated for 30 min. The color development was stopped by the addition of 0.36N H_2SO_4. Color intensity was determined with a microplate reader Model 680 (Bio-Rad Laboratories, Hercules, CA) at a wavelength of 450 nm with a reference wavelength of 620 nm. Analyte concentrations were calculated by referring to the standard curve using serial diluted recombinant MPF or MSLN, respectively (Fig. 2A for MPF and Fig. 2B for MSLN).

2.8. Statistical analyses

Nonparametric Mann Whitney's U test was used for comparison of the data. $p < 0.05$ was considered statistically significant. For drawing of receiver operating characteristic (ROC) curves and estimation of the area under the ROC curve (AUC) statistics software SPBS (Comworks, Saitama, Japan) was used to quantify the ability to differentiate

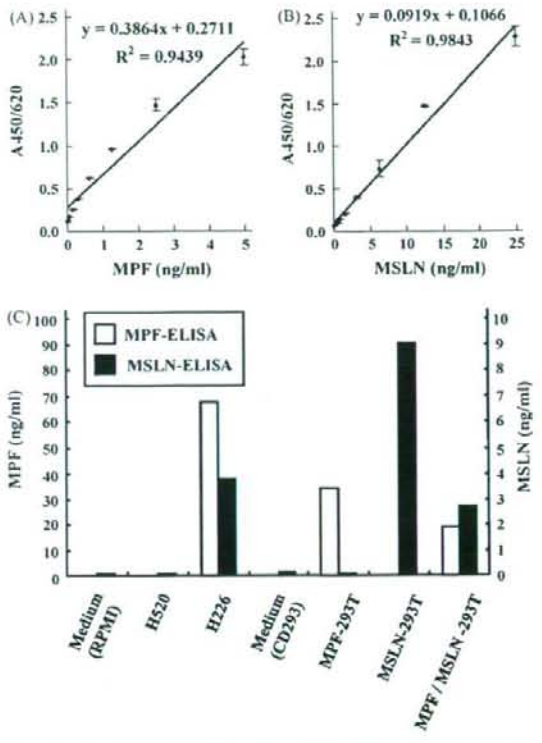

Fig. 2 Sandwich ELISA. Standard curves for MPF (A) and MSLN (B). ELISAs displaying the mean absorbance values from indicated concentrations of recombinant proteins. Points, mean; bars, S.D. (C), MPF and MSLN levels in the supernatants of cell lines and 293 transfectants measured by specific ELISA systems. The levels in the supernatants of 293 transfectants are indicated as those of 500 times diluted solution. Open bars, MPF; closed bars, MSLN.

between healthy volunteers and patients with indicated diseases. Pearson's correlation coefficient was calculated to determine the correlation between MPF and MSLN.

3. Results

3.1. Generation of sandwich ELISA specific for MPF and soluble mesothelin (MSLN)

To generate mAbs that specifically react with MPF, recombinant MPF protein corresponding to the amino acids 1–288 from the transcript variant 1 of human mesothelin was produced by 293T transfectants (Fig. 1A) and immunized to BALB/c mice. Supernatants of obtained hybridomas were tested for the binding activity to the microplate coated with immunizing antigen and further examined by a competition assay for the immunogen (data not shown). The specific reactivities of selected clone 20–10 and clone 41–28 to MPF were checked by immunoprecipitation using myc-His tagged recombinant MPF (Fig. 1B), and also performed by Western blot using the supernatants of 293T cells transfected with

expression vectors coding myc-His tagged MPF (Fig. 1C, lane 2) and the full length of mesothelin variant 1 (Fig. 1C, lane 3). A smaller band on lane 3 compared to the myc-His tagged MPF on lane 2 were detected by both anti-MPF Abs. MPF and mesothelin are produced together as a precursor form. Following cleavage by a protease furin, MPF is released as an N-terminal 31-kDa fragment from mesothelin [15]. The smaller band on the lane 3 seems to be the 31-kDa mature form of MPF without myc-His Tag. A sandwich ELISA for MPF was constructed using the anti-MPF antibodies 20–10 and 41–28. The standard curve using purified recombinant MPF was shown in Fig. 2A. Correlated with Fig. 1C, the MPF sandwich ELISA detected the antigen in the culture supernatant of the 293T transfectant expressing the full length of mesothelin variant 1 (Fig. 2C, MPF/MSLN-293T), as well as MPF-transfected cells (Fig. 2C, MPF-293T) but not the soluble mesothelin secreted in the culture supernatant of the MSLN-transfectants (Fig. 2C, MSLN-293T).

The monoclonal anti-MSLN antibody, clone 11–25, were generated by immunizing mice with recombinant MSLN (amino acids 297–580 of mesothelin variant 1). The specificity of 11–25 to MSLN was tested using a lung cancer cell line, NCI-H226, which has been clarified to express mesothelin [14]. 11–25 detected not only the antigen on the cell surface of NCI-H226 by flowcytometory (Fig. 1E, upper left panel), but also identified soluble antigen in the culture supernatant of NCI-H226 by immunoprecipitation (Fig. 1F, lane 11–25). Another anti-MSLN Ab, clone MN, which the Pastan's laboratory has previously developed, was used, in combination with 11–25, to establish a sandwich ELISA for MSLN [14]. The standard curve using recombinant MSLN was shown in Fig. 2B. The MSLN sandwich ELISA recognized the soluble antigen in the culture supernatant of NCI-H226 (Fig. 2C, H226) as well as the 293T transfectant expressing the full length of mesothelin variant1 (Fig. 2C, MPF/MSLN-293T). On the other hands, this MSLN ELISA did not detect recombinant MPF in the culture supernatant of the MPF-transfectants (Fig. 2C, MPF-293T).

3.2. MPF and MSLN in blood samples

We measured serum MPF and MSLN levels in all subjects. Serum MPF levels differed among the five groups (Fig. 3A and Table 1), with mean serum MPF values were higher for MPM patients (68.7 ± 101.1 ng/ml [mean ± standard deviation]) than for patients with lung cancer (16.6 ± 15.3 ng/ml), individuals with other cancers (15.1 ± 9.7 ng/ml), healthy asbestos-exposed subjects (9.7 ± 5.3 ng/ml) and healthy adults (9.0 ± 2.9 ng/ml). The difference in median values between MPM and every control group was statistically significant (Mann–Whitney's U test; $p < 0.001$). Mean serum MSLN levels in MPM, patients with lung cancer, individuals with other cancers, healthy asbestos-exposed subjects, or healthy adults were 130.0 ± 112.9 ng/ml, 83.4 ± 50.4 ng/ml, 74.4 ± 45.3 ng/ml, 59.5 ± 25.6 ng/ml and 61.4 ± 21.4 ng/ml, respectively (Fig. 3B and Table 1). The median serum MSLN level of MPM was significantly higher than in the control groups (Mann–Whitney's U test; MPM *vs.* lung cancer: $p = 0.028$, MPM *vs.* other cancers: $p = 0.005$, MPM *vs.* asbestos-exposed subjects: $p = 0.010$, MPM *vs.* healthy adults: $p < 0.001$). There was no significant difference in MPF or MSLN levels among MPM patients with different histologies (Table 1).

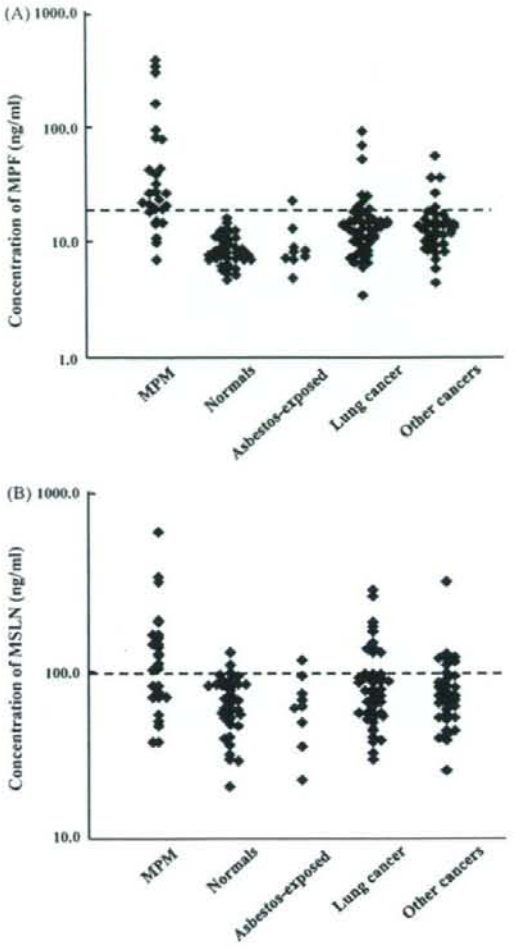

Fig. 3 Megakaryocyte potentiating factor (MPF) (A) and mesothelin variants (MSLN) (B) levels in the sera of malignant pleural mesothelioma (MPM) patients and control groups. Each dot represents one patient. The horizontal broken lines represent cut-off values: 19.1 ng/ml for MPF and 93.5 ng/ml for MSLN. MPM, malignant pleural mesothelioma; Normals, healthy volunteers; Asbestos-exposed, asbestos-exposed asymptomatic individuals; other cancers, ovarian, stomach and colon cancer patients.

3.3. Cut-off value, sensitivities and specificities calculation of MPF and MSLN

To assess the clinical potential of MPF, we compared sensitivities and specificities of MPF with those of MSLN. The operating characteristics for the two tumor markers with their cut-off points for achieving the best individual accuracy are shown in Fig. 4A. The area under the receiver operating characteristic (ROC) curve (AUC) for serum MPF

Table 1 Serum concentrations of megakaryocyte potentiating factor (MPF) and mesothelin variants (MSLN) in mesothelioma patients and controls

Diagnosis	Number of study participants	MPF (ng/ml)			MSLN (ng/ml)		
		Mean (S.D.)	Median	Range	Mean (S.D.)	Median	Range
MPM	27	68.7 (101.1)	26.3	6.9–370.1	130.0 (112.9)	101.5	35.9–576.1
Epithelial type	13	87.4 (112.6)	38.1	14.2–370.1	132.2 (67.7)	129.3	64.8–317.8
Sarcomatoid type	3	16.5 (5.8)	19.1	9.8–20.4	67.9 (38.6)	57.3	44.5–112.4
Mixed type	5	77.7 (143.7)	14.8	6.9–334.6	158.8 (233.6)	65.2	35.9–576.1
Unclassified type	6	47.0 (54.3)	24.7	15.3–156.3	132.3 (88.9)	109.7	35.9–296.6
Malignant condition							
Lung cancer	47	16.6 (15.3)	13.3*	3.4–89.4	83.4 (50.4)	70.7†	28.6–267.8
Other cancers	35	15.1 (9.7)	13.0*	4.4–54.5	74.4 (45.3)	66.4‡	24.6–298.2
Ovarian cancer	18	18.0 (12.5)	13.7	4.4–54.5	83.2 (56.9)	67.8	41.7–298.2
Stomach cancer	8	14.3 (3.7)	14.1	9.6–19.7	73.9 (29.0)	69.9	36.9–113.8
Colon cancer	9	9.7 (2.9)	8.7	5.8–14.0	57.0 (24.5)	51.6	24.6–106.6
Asbestos-exposed individuals	9	9.7 (5.3)	8.2*	4.9–22.7	59.5 (25.6)	56.7§	21.6–106.0
Healthy volunteers	38	9.0 (2.9)	8.0*	4.8–16.6	61.4 (21.4)	62.0*	19.6–117.4

* Significance of median values for the specified control groups compared with MPM. Mann–Whitney's *U* test; $p < 0.001$.
† Significance of median values for the specified control groups compared with MPM. Mann–Whitney's *U* test; $p = 0.028$.
‡ Significance of median values for the specified control groups compared with MPM. Mann–Whitney's *U* test; $p = 0.005$.
§ Significance of median values for the specified control groups compared with MPM. Mann–Whitney's *U* test; $p = 0.01$.

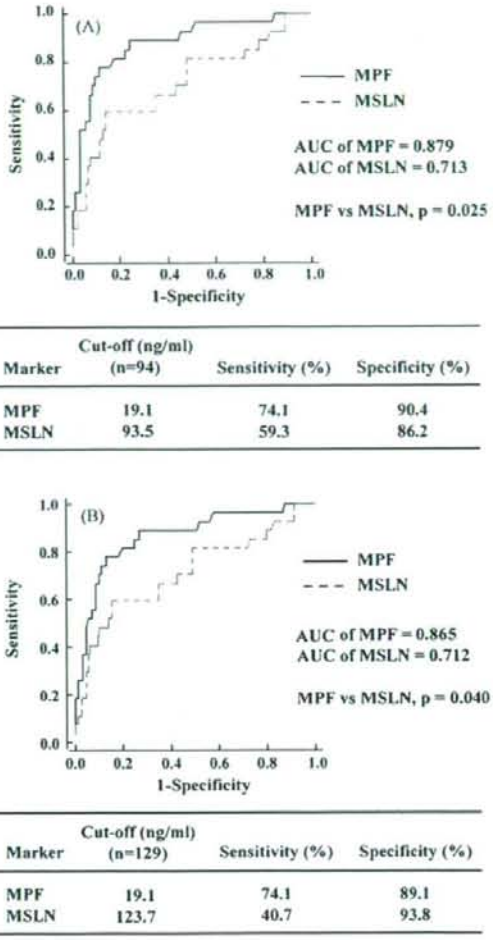

Marker	Cut-off (ng/ml) (n=94)	Sensitivity (%)	Specificity (%)
MPF	19.1	74.1	90.4
MSLN	93.5	59.3	86.2

Marker	Cut-off (ng/ml) (n=129)	Sensitivity (%)	Specificity (%)
MPF	19.1	74.1	89.1
MSLN	123.7	40.7	93.8

Fig. 4 Receiver operating characteristic (ROC) curves for megakaryocyte potentiating factor (MPF) and mesothelin variants (MSLN) for differentiation between malignant pleural mesothelioma ($n = 27$) and controls. Controls comprise lung cancer patients ($n = 47$), asbestos-exposed asymptomatic individuals ($n = 9$) and healthy volunteers ($n = 38$) for (A). For the analysis shown in (B), control groups include other cancers ($n = 35$) in addition to those specified in (A). The tables show the best statistical cut-off values for MPF and MSLN with pairs of sensitivity and specificity.

was 0.879 for differentiating MPM patients from controls comprising lung cancer patients, asbestos-exposed individuals and healthy adults, with a cut-off value of 19.1 ng/ml (sensitivity = 74.1%, specificity = 90.4%), whereas the AUC for serum MSLN was 0.713 with a cut-off value of 93.5 ng/ml (sensitivity = 59.3%, specificity = 86.2%) (Fig. 4A). Serum MPF levels were elevated in 20 (74.1%) MPM patients, eight (17.0%) lung cancer patients and five (14.3%) individuals with other cancers (Fig. 3A). Corresponding serum MSLN levels were elevated in 59.3%, 21.3% and 20.0% of the patients (Fig. 3B). Both MPF and MSLN showed elevated levels in

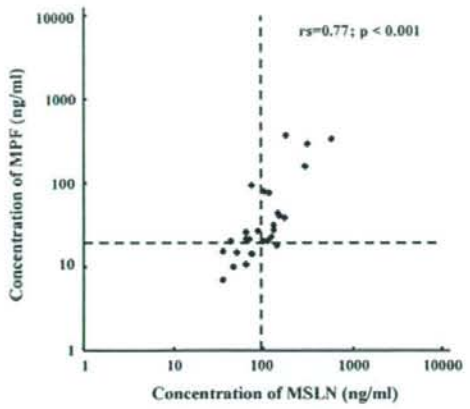

Fig. 5 Inter-marker correlation between megakaryocyte potentiating factor (MPF) and mesothelin variants (MSLN) for malignant pleural mesothelioma (MPM). Each dot indicates MPF and MSLN values for the same MPM patient ($n = 27$). r_s, Pearson's correlation coefficient. The horizontal dotted line represents the cut-off value for MPM (19.1 ng/ml) and the vertical dotted line for MSLN (93.5 ng/ml).

four (22.2%) ovarian cancer patients, while MPF values were elevated in one (11.1%) asbestos-exposed adult and none of the healthy donors, and MSLN levels were elevated in one (11.1%) asbestos-exposed adult and two (5.3%) healthy donors. Calculation of areas under the ROC curves showed a significant difference between the two markers ($p = 0.025$) (Fig. 4A). ROC curves for a comparison of MPM with all non-MPM patients and healthy adults, yielded an AUC of 0.865 for MPF and of 0.712 for MSLN (MPF *vs.* mesothelin, $p = 0.04$) (Fig. 4B). Sensitivity of MSLN decreased to 40.7% while that of MPF did not change (Fig. 4B). Comparison of the AUC values thus showed a better diagnostic performance by MPF than MSLN for discriminating MPM.

3.4. Inter-marker correlation

To examine inter-marker correlation between MPF and MSLN values for MPM, we plotted concentrations of MPF and MSLN in the same figure (Fig. 5) and found a significant correlation between MPF and MSLN values for MPM (Pearson's correlation coefficient, $r_s = 0.77$; $p < 0.001$). Concentrations for six patients were above the cut-off value for MPF (19.1 ng/ml) but below the cut-off values (93.5 ng/ml) for MSLN, whereas only one showed the opposite condition. Concentrations for 14 patients were above the cut-off values for both markers and for six patients they were below these values (Fig. 5).

4. Discussion

Recent studies identified increased levels of MSLN in the blood of MPM [11,16–18] and other histological cancer patients [9,10]. They suggested MSLN was useful for diagnosis of MPM and for monitoring disease progression. Recently, MPM patients were found to have raised serum concentrations of MPF [13,19], indicating that MPF can also be a candidate diagnostic marker for MPM. To determine which molecule, MPF or MSLN, is more sensitive for screening of MPM, we developed two novel sets of ELISA system. The one for MSLN recognizes mesothelin variants 1 and 3. In our study, higher MPF levels were found in 74.1% of MPM patients and elevated MSLN levels in 59.3%. Scherpereel et al. demonstrated that MPM epithelioid type had significant elevated values for MSLN than mixed type or sarcomatoid type [17]. Nevertheless, we and Creaney et al. did not find significant difference in levels of either MSLN or MPF in MPM patients with different histologies (Table 1) [20]. The sensitivity of 59.3% of MSLN established in our study was comparable to the sensitivity of 52% in Creaney' s study of 117 MPM patients [20] or 68% of Cristaudo' s study [21]. Regarding sensitivity of MPF to patients with MPM, we do not know any other reports.

When two or more tests are available for diagnostic purposes, comparison of the respective AUCs will often show which test is the most effective. ROC curves of MPF yielded an AUC of 0.879, and those of MSLN an AUC of 0.713 (MPF *vs.* MSLN, $p = 0.025$) (Fig. 4A). There was a significant correlation between MPF an MSLN values for MPM (Pearson's correlation coefficient (r_s) = 0.77). This indicates that MPF is probably more sensitive than MSLN for diagnosis of MPM. Though osteopontin and CA125 are also indicated as potential markers in the diagnosis of MPM, neither showed better sensitivity for MPM in comparison with MSLN [20,22].

Physiological cleavage from the mesothelin precursor protein at the furin cleavage site may be responsible for extracellular secretion of MPF [13]. Mesothelin and its variants, attached to cell membranes by GPI-anchors, are also readily released *in vivo*, but the mechanism of mesothelin release has not yet been identified. We transfected the full length of mesothelin variant 1 cDNA into 293 cells and part of mesothelin variant 1 is released from the cell surface and can be measured with the ELISA system (Fig. 2 C, MPF/MSLN-293T). A relevant example is carcinoembryonic antigen (CEA), a tumor-associated GPI-anchored glycoprotein that is commonly shed from the cell surface [23]. The as yet unknown process that mediates a release of the membrane-bound mesothelin variant 1 may be associated with the lower sensitivity of MSLN in comparison with that of MPF. However, additional studies are needed to identify and characterize the process of mesothelin secretion.

Just as MPF and mesothelin originate from the same mesothelin precursor, so adrenomedullin (ADM) and proadrenomedulin (PAMP) are potent vasodilatory peptides derived from a common precursor peptide. However, their short half-life and the presence of a binding protein have been obstacles for an accurate quantification. The ADM precursor is produced in quantities stoichiometric to ADM and PAMP, but is non-functional and stable, while the quantities of the ADM precursor thus produced directly reflect those of ADM and PAMP [24]. One of the reasons for the lower sensitivity of the mesothelin assay could be a lower stability of the protein, but the stability of both proteins needs to be examined and compared.

Pastan's group showed that most ovarian cancer cells express 40-kDa protein mesothelin at the cell surface [25]. MPF was initially isolated from supernatant of pancreatic

cancer cells [26]. Scholler et al. and Hassan et al. independently demonstrated elevated levels of SMRP in 23 of 30 (76.7%) and 40 of 56 (71%) sera from patients with ovarian carcinoma by using a monoclonal antibody, OV569, that was prepared by immunizing mice with ovarian carcinoma cells [10,18]. However, Beyer et al. reported SMRP values were increased in less than 10% of 111 samples collected from ovarian cancer patients [16]. In our study, serum concentrations of both MPF and MSLN were increased in only four of 18 (22.2%) individuals with ovarian cancer. Frequent positive immunostaining for mesothelin is reportedly associated with the non-mucinous type of ovarian cancers [27,28]. Although these reports did not include a description of histological subtype classification in the various blood samples studied, the different ratios of mucinous to non-mucinous type in the samples may partly account for the differences in positivity of serum mesothelin. For MPF, ours is the first reported study of serum levels in ovarian cancer patients.

5. Conclusion

We used ELISA systems developed by us to detect significant differences in the levels of serum MPF and MSLN between MPM patients and controls including lung cancer patients, asbestos-exposed individuals, and normal volunteers. In addition, it is suggested that MPF has superior specificity for MPM compared to MSLN. We are planning a further study to determine the relationship between serum MPF and disease stage, prognosis and histological subtypes.

Conflict of interest

None.

Acknowledgements

The following medical institute and investigator was involved in the study: The First Department of Internal Medicine, Faculty of Medicine, University of Toyama (Ryuji Hayashi).

References

[1] Vogelzang NJ, Rusthoven JJ, Symanowski J, Denham C, Kaukel E, Ruffie P, et al. Phase III study of pemetrexed in combination with cisplatin versus cisplatin alone in patients with malignant pleural mesothelioma. J Clin Oncol 2003;21:2636–44.
[2] Stahel RA. Malignant pleural mesothelioma: a new standard of care. Lung Cancer 2006;54(Suppl 2):S9–14.
[3] Pelucchi C, Malvezzi M, La Vecchia C, Levi F, Decarli A, Negri E. The Mesothelioma epidemic in Western Europe: an update. Br J Cancer 2004;90:1022–4.
[4] Leithner K, Leithner A, Clar H, Weinhaeusel A, Radl R, Krippl P, et al. Mesothelioma mortality in Europe: impact of asbestos consumption and simian virus 40. Orphanet J Rare Dis 2006;1:44.
[5] Murayama T, Takahashi K, Natori Y, Kurumatani N. Estimation of future mortality from pleural malignant mesothelioma in Japan based on an age-cohort model. Am J Ind Med 2006;49:1–7.
[6] Leigh J, Driscoll T. Malignant mesothelioma in Australia, 1945–2002. Int J Occup Environ Health 2003;9:206–17.
[7] Chang K, Pastan I. Molecular cloning of mesothelin, a differentiation antigen present on mesothelium, mesotheliomas, and ovarian cancers. Proc Natl Acad Sci USA 1996;93:136–40.
[8] Muminova ZE, Strong TV, Shaw DR. Characterization of human mesothelin transcripts in ovarian and pancreatic cancer. BMC Cancer 2004;4:19.
[9] Hellstrom I, Raycraft J, Kanan S, Sardesai NY, Verch T, Yang Y, et al. Mesothelin variant 1 is released from tumor cells as a diagnostic marker. Cancer Epidemiol Biomarkers Prev 2006;15:1014–20.
[10] Scholler N, Fu N, Yang Y, Ye Z, Goodman GE, Hellstrom KE, et al. Soluble member(s) of the mesothelin/megakaryocyte potentiating factor family are detectable in sera from patients with ovarian carcinoma. Proc Natl Acad Sci USA 1999;96:11531–6.
[11] Robinson BW, Creaney J, Lake R, Nowak A, Musk AW, de Klerk N, et al. Mesothelin-family proteins and diagnosis of mesothelioma. Lancet 2003;362:1612–6.
[12] Shiomi K, Miyamoto H, Segawa T, Hagiwara Y, Ota A, Maeda M, et al. Novel ELISA system for detection of N-ERC/mesothelin in the sera of mesothelioma patients. Cancer Sci 2006;97:928–32.
[13] Onda M, Nagata S, Ho M, Bera TK, Hassan R, Alexander RH, et al. Megakaryocyte potentiation factor cleaved from mesothelin precursor is a useful tumor marker in the serum of patients with mesothelioma. Clin Cancer Res 2006;12:4225–31.
[14] Onda M, Willingham M, Nagata S, Bera TK, Beers R, Ho M, et al. New monoclonal antibodies to mesothelin useful for immunohistochemistry, fluorescence-activated cell sorting, Western blotting, and ELISA. Clin Cancer Res 2005;11:5840–6.
[15] Hassan R, Bera T, Pastan I. Mesothelin: a new target for immunotherapy. Clin Cancer Res 2004;10:3937–42.
[16] Beyer HL, Geschwindt RD, Glover CL, Tran L, Hellstrom I, Hellstrom KE, et al. MESOMARK: a potential test for malignant pleural mesothelioma. Clin Chem 2007;53:666–72.
[17] Scherpereel A, Grigoriu B, Conti M, Gey T, Gregoire M, Copin MC, et al. Soluble mesothelin-related peptides in the diagnosis of malignant pleural mesothelioma. Am J Respir Crit Care Med 2006;173:1155–60.
[18] Hassan R, Remaley AT, Sampson ML, Zhang J, Cox DD, Pingpank J, et al. Detection and quantitation of serum mesothelin, a tumor marker for patients with mesothelioma and ovarian cancer. Clin Cancer Res 2006;12:447–53.
[19] Maeda M, Hino O. Molecular tumor markers for asbestos-related mesothelioma: serum diagnostic markers. Pathol Int 2006;56:649–54.
[20] Creaney J, van Bruggen I, Hof M, Segal A, Musk AW, de Klerk N, et al. Combined CA125 and mesothelin levels for the diagnosis of malignant mesothelioma. Chest 2007;132:1239–46.
[21] Cristaudo A, Foddis R, Vivaldi A, Guglielmi G, Dipalma N, Filiberti R, et al. Clinical significance of serum mesothelin in patients with mesothelioma and lung cancer. Clin Cancer Res 2007:5076–81.
[22] Grigoriu BD, Scherpereel A, Devos P, Chahine B, Letourneux M, Lebailly P, et al. Utility of osteopontin and serum mesothelin in malignant pleural mesothelioma diagnosis and prognosis assessment. Clin Cancer Res 2007;13:2928–35.
[23] Khan WN, Hammarstrom S. Biosynthesis of carcinoembryonic antigen (CEA) gene family members expressed in human tumor cell lines: evidence for cleavage of the glycosyl phosphatidyl inositol (GPI) anchor by GPI-PLC and GPI-PLD. Biochem Int 1991;25:723–31.
[24] Ernst A, Hellmich S, Bergmann A. Proneurotensin 1–117, a stable neurotensin precursor fragment identified in human circulation. Peptides 2006;27:1787–93.
[25] Chang K, Pai LH, Batra JK, Pastan I, Willingham MC. Characterization of the antigen (CAK1) recognized by monoclonal

antibody K1 present on ovarian cancers and normal mesothelium. Cancer Res 1992;52:181–6.
[26] Yamaguchi N, Hattori K, Oh-eda M, Kojima T, Imai N, Ochi N. A novel cytokine exhibiting megakaryocyte potentiating activity from a human pancreatic tumor cell line HPC-Y5. J Biol Chem 1994;269:805–8.
[27] Chang K, Pastan I, Willingham MC. Isolation and characterization of a monoclonal antibody, K1, reactive with ovarian cancers and normal mesothelium. Int J Cancer 1992;50: 373–81.
[28] Ordonez NG. Application of mesothelin immunostaining in tumor diagnosis. Am J Surg Pathol 2003;27:1418–28.

Pathology International 2008; **58**: 253–256 doi:10.1111/j.1440-1827.2008.02220.x

Short Communication

Pleural MALT lymphoma diagnosed on thoracoscopic resection under local anesthesia using an insulation-tipped diathermic knife

Kunimitsu Kawahara,[1] Shinji Sasada,[2] Teruaki Nagano,[1] Hidekazu Suzuki,[2] Masashi Kobayashi,[2] Kaoru Matsui,[2] Katsuyoshi Takata,[3] Tadashi Yoshino,[3] Tomoki Michida[4] and Teruo Iwasaki[5]

Departments of [1]Pathology, [2]Thoracic Malignancy and [5]Respiratory Surgery, Osaka Prefectural Medical Center for Respiratory and Allergic Diseases, Habikino, [3]Department of Pathology, Okayama University Graduate School of Medicine, Dentistry and Pharmaceutical Sciences, Okayama and [4]Department of Internal Medicine, Osaka Koseinenkin Hospital, Osaka, Japan

A 79-year-old man presented with back pain. Chest CT scan showed elevated nodular lesions in the right parietal pleurae with pleural effusion. There were no intrapulmonary or mediastinal abnormalities. Under local anesthesia, right thoracoscopy and subsequent thoracoscopic pleural resection were performed using an insulation-tipped diathermic knife (IT-knife). The resected pleura, 2.2 cm in diameter, had a rough granular surface. Lymphoid cells histologically infiltrated diffusely into the pleura. They were composed of centrocyte-like and monocytoid cells. On immunohistochemistry they were found to be positive for Bcl2, CD20, CD45RB and CD79a, but negative for CD3, CD5, CD10 and cyclin D1. EBV-encoded small RNA-1 (EBER-1) *in situ* hybridization was negative. A diagnosis of extranodal marginal zone B-cell lymphoma of mucosa-associated lymphoid tissue (MALT lymphoma) arising in the pleura was therefore made. To the authors' knowledge this is the first case in which IT-knife was used for diagnosis of a pleural lesion. This large, single-piece, only slightly crushed pleural specimen, enabled study of histopathological findings (listed here) that could not have been obtained on conventional biopsy: (i) lack of apparent evidence of plasmacytic differentiation; (ii) no recognition of lymphoid follicles; (iii) mesothelial cells not infiltrated by lymphoma cell clusters; (iv) thin layer of hyperplastic mesothelial cells continuously covering the surface; and (v) no proliferation of fibroblast-like submesothelial cells.

Key words: insulation-tipped diathermic knife, MALT lymphoma, pleura, thoracoscopy

Correspondence: Kunimitsu Kawahara, MD, PhD, Department of Pathology, Osaka Prefectural Medical Center for Respiratory and Allergic Diseases, 3-7-1 Habikino, Habikino-shi, Osaka 583-8588, Japan. Email: kawahara@hbk.pref.osaka.jp

Received 18 August 2007. Accepted for publication 20 November 2007.

Extranodal marginal zone B-cell lymphoma of mucosa-associated lymphoid tissue (MALT lymphoma) arising in the pleura is extremely rare, with only four published cases.[1–3] Reported cases were diagnosed pathologically using surgically resected pleural specimen under thoracotomy[1,3] or under video-assisted thoracic surgery (VATS).[2] But in these cases the histopathological findings were not described in detail, probably because the obtained specimens were fragmented or highly crushed. To resolve these issues, large, single-piece and only slightly crushed resected specimens are necessary.

In Japan, endoscopic mucosal resection (EMR) of gastric mucosa by gastrointestinal endoscopists has been accepted as a treatment option for early gastric cancer (EGC).[4] For resection of larger EGC as a single-piece specimen, a new EMR method using an insulation-tipped diathermic knife (IT-knife; Olympus, Tokyo, Japan) was developed.[4–6]

Herein we present the first case of pleural MALT lymphoma that was diagnosed thoracoscopically using a large and single-piece specimen obtained using an IT-knife (thoracoscopic IT-knife) and describe the histopathological findings of pleural MALT lymphoma in detail.

CASE REPORT

Clinical history

A 79-year-old man who had smoked approximately 60 cigarettes per day for 40 years, consulted Osaka Prefectural Medical Center for Respiratory and Allergic Diseases complaining of back pain that had persisted for 2 months. Family

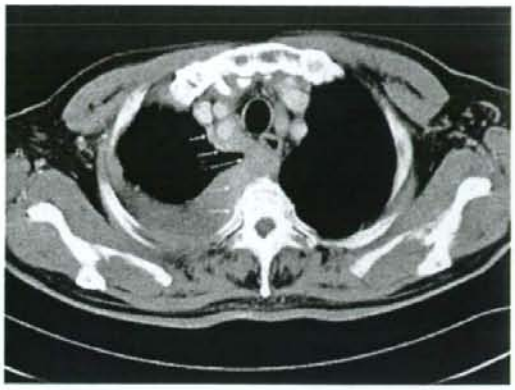

Figure 1 Chest CT scan showing diffuse prominent thickening of right mediastinal pleura (arrows) and pleural effusion.

history, past medical history and occupational history were unremarkable. Chest CT scan (Fig. 1) showed diffuse prominent thickening of the right mediastinal and costal pleurae. Right pleural effusion was present but there were no intrapulmonary or mediastinal abnormalities. Pleural effusion cytology did not show any evidence of neoplasia. Laboratory tests and CT scan of the abdomen and pelvis were unremarkable. Serum CEA, neuron-specific enolase, cytokeratin-19 fragment and soluble interleukin-2-receptor levels were 4.7 ng/mL (cut-off: 5 ng/mL) , 10.4 ng/mL (cut-off: 10 ng/mL), 1.3 ng/mL (cut-off: 3.5 ng/mL) and 857 U/mL (cut-off: 466 U/mL), respectively. A tentative diagnosis of pleural malignant mesothelioma was made. After removal of 1340 mL of pleural effusion, a thoracoscopic IT-knife was used to resect a nodular lesion in the costal parietal pleura under local anesthesia (Fig. 2a,b).

Macroscopic findings

The resected pleura measured 2.2 cm in diameter and had a rough granular surface (Fig. 2c). The specimen was serially examined at 4 mm intervals. The cut surface (Fig. 2d) was whitish and exhibited prominent thickening of the pleura.

Microscopic findings

Throughout the whole pleural specimen, from the superficial submesothelial layer to the deep margin, a diffuse infiltrate of small- to -medium lymphoid cells was recognized (Fig. 3a). These cells were composed of centrocyte-like and monocytoid cells (Fig. 3b). Plasmacytic differentiation was inconspicuous and lymphoid follicles were absent (Fig. 3b).

Figure 4 Clonal polymerase chain reaction (PCR). Clonal analysis of immunoglobulin heavy-chain (*IgH*) gene rearrangements was performed using semi-nested PCR. Lane 1, negative control; lane 2, positive control; lane 3, reactive lymphoid hyperplasia; lane 4, present case; lane 5, present case. Two samples (lanes 4, 5) taken from the right costal pleurae had a distinct single clonal band in the PCR assay for the *IgH* gene.

Mitoses were present in 3 figures/50 high-power fields. There was no necrosis or hemorrhage. Immunohistochemistry showed that these cells were positive for Bcl2, CD20, CD45RB and CD79a (Fig. 3c), but negative for CD3, CD5, CD10 and cyclin D1. EBV-encoded small RNA-1 (EBER-1) *in situ* hybridization was negative. Therefore, we made a final diagnosis of pleural MALT lymphoma. AE1/AE3 staining showed that the pleural lesions were covered with a thin continuous layer of hyperplastic mesothelial cells (Fig. 3d), but there was no infiltration of lymphoma cell clusters among the mesothelial cells, like the lymphoepithelial lesions typically seen in gastric lesions (Fig. 3e). There was no proliferation of submesothelial fibroblast-like cells (Fig. 3e).

Clonal analysis by polymerase chain reaction

Clonality analysis of immunoglobulin heavy-chain (*IgH*) gene rearrangements was performed using semi-nested polymerase chain reaction (PCR). The PCR conditions and the primers used (FR2A, LJH and VLJH) have been described previously.[7,8] This case had a distinct single clonal band in the PCR assay for the *IgH* gene (Fig. 4).

DISCUSSION

MALT lymphoma is an extranodal indolent lymphoma consisting of morphologically heterogenous small B-cells: marginal zone (centrocyte-like) cells, monocytoid cells, small lymphocytes, and scattered immunoblasts and centroblast-like cells.[9] The gastrointestinal tract is the most common site.[9] In the present case a diffuse infiltrate of small- to -medium lymphoid cells was recognized in the pleural specimens. Plasmacytic differentiation was inconspicuous and

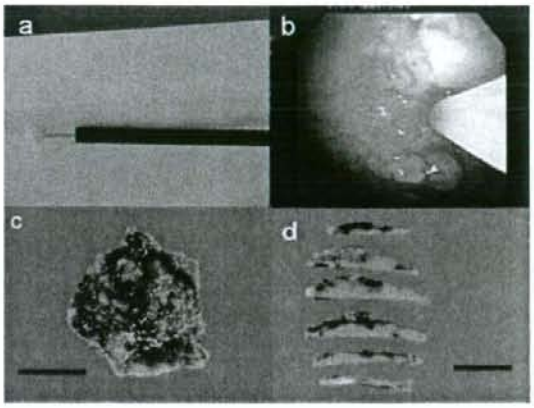

Figure 2 (**a**) Insulated-tipped diathermic knife (IT-knife): Needle knife with a ceramic ball at the top. (**b**) Thoracoscopic image showing a nodular lesion in the parietal pleura being incised. (**c**) Resected pleura with a rough granular surface. Bar, 1 cm (**d**) Cut surface showing prominent thickening of the pleura and a whitish appearance. Bar, 1 cm.

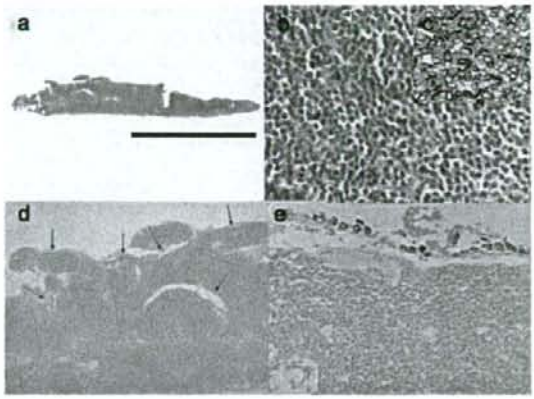

Figure 3 (**a**) Diffuse infiltrate of lymphoid cells through all layers of the pleura. Bar, 1 cm (**b**) Tumor cells composed of centrocyte-like and monocytoid lymphoid cells without apparent plasmacytic differentiation or follicular formation. (**c**) CD79a staining showing positivity for most tumor cells. (**d**) AE1/AE3 staining: thin layer of hyperplastic mesothelial cells (arrows). These cells covered the surfaces of pleural granular lesions. (**e**) AE1/AE3 staining did not show any proliferation of submesothelial fibroblast-like cells.

lymphoid follicles were completely absent histologically. These microscopic features also indicated another possibility of mature B-cell neoplasms including follicular lymphoma and mantle cell lymphoma. Most cases of follicular lymphoma are composed of small to medium-sized cells (centrocytes) and large transformed cells (centroblasts).[10] Large cell components were absent in the present case. Immunohistochemically, these tumor cells of follicular lymphoma are usually positive for CD10,[10] but this was negative in the present case. The neoplastic cells of mantle cell lymphoma are composed of small to medium-sized lymphoid cells most closely resembling centrocytes.[11] They are typically CD5 and cyclin D1 positive,[11] but in the present case these two markers were negative.

Until recently, MALT lymphoma primarily involving the pleura had not been documented, until Ahmad *et al.*[2] reported the first two cases of pleural MALT lymphoma; an additional two cases were reported thereafter.[1,3] Of four